PRIMARY RESEARCH ARTICLE

WILEY · Global Change Biology

Resilience of tropical tree cover: The roles of climate, fire, and herbivory

Arie Staal[1] [iD] | Egbert H. van Nes[1] | Stijn Hantson[2] | Milena Holmgren[3] |
Stefan C. Dekker[4,5] | Salvador Pueyo[6] | Chi Xu[7] | Marten Scheffer[1] [iD]

[1]Aquatic Ecology and Water Quality Management Group, Department of Environmental Sciences, Wageningen University, Wageningen, The Netherlands

[2]Department of Earth System Science, University of California, Irvine, California 92697

[3]Resource Ecology Group, Department of Environmental Sciences, Wageningen University, Wageningen, The Netherlands

[4]Department of Environmental Sciences, Copernicus Institute for Sustainable Development, Utrecht University, Utrecht, The Netherlands

[5]Faculty of Management, Science and Technology, Open University, Heerlen, The Netherlands

[6]Department of Evolutionary Biology, Ecology and Environmental Sciences, Universitat de Barcelona, Barcelona, Spain

[7]School of Life Sciences, Nanjing University, Nanjing, China

Correspondence
Arie Staal, Aquatic Ecology and Water Quality Management Group, Department of Environmental Sciences, Wageningen University, Wageningen, The Netherlands.
Email: ariestaal@gmail.com

Abstract

Fires and herbivores shape tropical vegetation structure, but their effects on the stability of tree cover in different climates remain elusive. Here, we integrate empirical and theoretical approaches to determine the effects of climate on fire- and herbivore-driven forest-savanna shifts. We analyzed time series of remotely sensed tree cover and fire observations with estimates of herbivore pressure across the tropics to quantify the fire–tree cover and herbivore–tree cover feedbacks along climatic gradients. From these empirical results, we developed a spatially explicit, stochastic fire-vegetation model that accounts for herbivore pressure. We find emergent alternative stable states in tree cover with hysteresis across rainfall conditions. Whereas the herbivore–tree cover feedback can maintain low tree cover below 1,100 mm mean annual rainfall, the fire–tree cover feedback can maintain low tree cover at higher rainfall levels. Interestingly, the rainfall range where fire-driven alternative vegetation states can be found depends strongly on rainfall variability. Both higher seasonal and interannual variability in rainfall increase fire frequency, but only seasonality expands the distribution of fire-maintained savannas into wetter climates. The strength of the fire–tree cover feedback depends on the spatial configuration of tree cover: Landscapes with clustered low tree-cover areas are more susceptible to cross a tipping point of fire-driven forest loss than landscapes with scattered deforested patches. Our study shows how feedbacks involving fire, herbivores, and the spatial structure of tree cover explain the resilience of tree cover across climates.

KEYWORDS
alternative stable states, bistability, forest, grasslands, livestock, model, regime shifts, remote sensing, tipping points, wildfire

1 | INTRODUCTION

Large-scale analyses of the frequency distributions of tropical tree cover indicate that forests and savannas can be alternative stable states (Hirota, Holmgren, van Nes, & Scheffer, 2011; Staver, Archibald, & Levin, 2011; Xu et al., 2016). Moreover, they show that savannas become more common with decreasing average rainfall

(Hirota et al., 2011; Staver et al., 2011), increasing seasonality (Staal, Dekker, Xu, & van Nes, 2016), and increasing interannual variability of rainfall (Holmgren, Hirota, van Nes, & Scheffer, 2013). The key to identify alternative stable states is to understand the positive feedbacks that may generate them. If positive feedbacks are sufficiently strong, they can maintain alternative stable states. This implies hysteresis: For different initial conditions, the system may end up in different end states under the same environmental conditions. Alternative stable states are usually separated by tipping points (sensu Van Nes et al., 2016). Away from tipping points, relatively large environmental changes may have small effects, but close to tipping points, even small changes in an environmental factor can produce a shift that is hard to reverse (Scheffer, Carpenter, Foley, Folke, & Walker, 2001).

Several recent theoretical (e.g., Lasslop, Brovkin, Reick, Bathiany, & Kloster, 2016; Schertzer, Staver, & Levin, 2015; Staver & Levin, 2012; Van Nes, Hirota, Holmgren, & Scheffer, 2014) and empirical advances (e.g., D'Onofrio, von Hardenberg, & Baudena, 2018; Dantas, Hirota, Oliveira, & Pausas, 2016; Flores et al., 2017; Hoffmann et al., 2012; Murphy & Bowman, 2012; Staver et al., 2011; Van Nes et al., 2018) support the hypothesis that fire-vegetation feedbacks provide one of the dominant mechanisms explaining the main patterns of tree-cover distributions across the tropics. The continuous grass layers that characterize tropical savannas fuel fires which, in turn, enhance landscape openness and grass growth by killing trees or removing their aboveground biomass; on the other hand, closed forest canopies suppress fires, thereby contributing to maintain a tree-dominated closed landscape (Murphy & Bowman, 2012; Van Nes et al., 2018).

Not only fire, but also herbivory, is an important factor that affects tree cover, especially in arid savannas (Archibald & Hempson, 2016; Sankaran et al., 2005). Different functional groups of herbivores have different effects on tree cover. Grazers feed on grass, whereas browsers, as well as mixed feeders (consuming both grasses and woody plants), may feed on young tree seedlings and saplings limiting tree cover (Sankaran, Ratnam, & Hanan, 2008). This browsing effect of herbivores introduces a feedback with tree cover analogous to the one with fire: By suppressing tree growth in its juvenile stages, herbivores may maintain a low-tree-cover landscape that supports more herbivores than a closed canopy landscape (Dantas et al., 2016; Staver & Bond, 2014). The dominant form of herbivory in the tropics is livestock herbivory (Hempson, Archibald, & Bond, 2015; Oesterheld, Sala, & McNaughton, 1992), which includes browsers and mixed feeders (Robinson et al., 2014). Even in Africa, where many natural herbivores are still present, livestock are the most widespread and abundant herbivores (Hempson et al., 2015).

Predicting how feedbacks may change the stability of tropical forests and savannas in a future with stronger and more frequent climatic extremes (Bathiany, Dakos, Scheffer, & Lenton, 2018; Huang, Xie, Hu, Huang, & Huang, 2013) is an urgent challenge. To better understand the emergent effects of feedbacks between fire, herbivores, and tree cover, we need a modeling framework that can well integrate spatial dynamics (DeAngelis & Yurek, 2017) across rainfall

gradients. Small-scale theoretical models, including spatially explicit ones (e.g., Schertzer et al., 2015), have been used to study complex fire dynamics, but they lack a large-scale quantification of the complete feedback loop. Meanwhile, large-scale observation-based models, such as global fire-vegetation models (Hantson et al., 2016), do not account for the small-scale dynamics that generate observed fire- and tree-cover patterns (Pausas & Dantas, 2017). To bridge this gap, we present a spatially explicit fire model that is parameterized on time series of remotely sensed tree-cover and fire observations from across the tropics. We quantify from these observations the fire–tree cover feedback loop and determine the effects of rainfall variability on fire frequencies. Similarly, we quantify the herbivore–tree cover feedback loop through estimated livestock densities across the rainfall gradient.

We test whether and how our parameterized model predicts tipping points in tropical tree cover. More specifically, given the poorly understood effects of intensifications of rainfall variability due to climate change (Boisier, Ciais, Ducharne, & Guimberteau, 2015; Huang et al., 2013) and land-use changes (Staal et al., 2018) on fire dynamics, we use the model to investigate how increasing rainfall variability may affect the stability and resilience of tree cover in tropical ecosystems.

2 | MATERIALS AND METHODS

In our description of the model structure and design, we follow the Overview, Design concepts, and Details (ODD) protocol by Grimm et al. (2006). According to this protocol, the model description is separated into seven parts: "Purpose", "State variables and scales", "Process overview and schedule", "Design concepts", "Initializations and perturbations", "Input data", and "Submodels".

2.1 | Purpose

The purpose of the model is to study how feedbacks between tree cover and fire, and between tree cover and herbivory, affect the stability of tree cover across climatic gradients in tropical and subtropical South America, Africa, Australia, and Asia, between 15°N and 35°S. To meet that purpose, the model is spatially explicit and empirically parameterized using remotely sensed data.

2.2 | State variables and scales

The state variable of the model is tree cover T (%). The model is spatially explicit, implemented on a square lattice of 100×100 cells with periodic boundaries (i.e., the lattice boundaries are connected). In each cell, tree-cover dynamics are described by a difference equation. The spatial resolution is the same as that of the remotely sensed tree-cover data (250×250 m), so the lattice represents a landscape of 25×25 km. Each cell in the lattice contains information about tree cover in a given time step of 1 year and whether or not the cell is burning. Within each time step, a new fire can ignite in any cell and subsequently spread to any of a burning cell's eight neighboring cells according to empirically obtained fire probabilities

(see "Fire probabilities" and "Fire ignition and spread" under "Submodels"). Fire spreads within a time step, because fire spread is assumed to take place on a much faster time scale than growth (Pueyo, 2007).

2.3 | Process overview and schedule

The model includes an empirical growth term and a fire-induced loss term of tree cover. The growth term, G(MAR, T, H), is a function of mean annual rainfall (MAR), tree cover (T), and herbivore density (H). The fire-induced loss term, $F(T, R, V)$, is an empirical function of tree cover, rainfall in a given year (R), and rainfall variability (V). This gives the following structure of the model for tree cover in column elements i and row elements j:

$$T_{ij}(t+1) = T_{ij}(t) + G_{ij}(MAR, T, H)(t) - F_{ij}(T, R, V)(t) \qquad (1)$$

where rainfall variability V is separated into seasonality S and interannual variability I.

2.4 | Design concepts

We focus on modeling feedbacks of tree cover with fire and herbivory. Any alternative stable states in tree cover are an emergent property of the model. The fire component of the model is stochastic in discrete events, whereas the herbivory component is deterministic and constant. This reflects the fundamental difference in the way those two processes exert pressure on tree cover (Archibald & Hempson, 2016).

2.5 | Initializations and perturbations

Two ways of initializing the model were performed: (a) To validate the model, we repeated the following analysis 10,000 times: We selected one random location (250 × 250 m) in the tropics and used the observed tree cover, mean annual rainfall, and rainfall seasonality in that location (see "Input data" for details of the data) as initial conditions homogeneously in the whole lattice and simulated 1,000 years. We used linear regression to evaluate the correspondence between observed tree cover and the model-predicted stabilized tree cover. (b) To systematically test under which climates the model generates alternative stable states in tree cover, we set either homogeneous high tree cover (80%; "forest") or homogeneous low tree cover (10%; "savanna") as initial conditions. Climates that were considered were all mean annual rainfall levels between 0 and 2,000 mm/year in intervals of 10 mm/year, in each case for all combinations of 0–3 standard deviations in rainfall seasonality and 0–3 standard deviations in interannual rainfall variability from the average (see "Input data").

We tested the resilience of the tree-cover states by initializing the lattice as high tree cover (low tree cover) and by subsequently setting an increasingly large proportion of cells (up to the entire lattice) to low tree cover (high tree cover). We simulated 1,000 years and recorded the resulting average tree cover. Two types of spatial

perturbation were tested: clustered perturbations and random perturbations. For the clustered perturbations, we imposed the perturbation as a square area of cells; for the random perturbations, the location of each perturbed cell was randomly assigned across the lattice. We present results for mean annual rainfall levels of [1,300, 1,400, … 1,700] mm/year under average rainfall variability and for 1,700 mm/year for up to three standard deviations of rainfall seasonality above the average.

We also explored how burned area depends on tree cover and rainfall conditions, for which we systematically experimented through a number of runs, each time with constant tree cover [5%, 15%, … 85%], rainfall [100, 200, … 2,000], and seasonality (0–3 standard deviations from the average). In each run, we recorded all fires and their sizes and determined burned area. Here, we performed runs of 5,000 years instead of 1,000 years to allow for a more representative picture under conditions where fires are rare.

2.6 | Input data

We used climatic and satellite data to parameterize the model and to initialize the simulation runs. Tree-cover data were extracted from the MODIS VCF Collection 5 dataset for the years 2001–2010 (DiMiceli et al., 2011) at 250-m resolution. Monthly rainfall data were downloaded from the Climate Research Unit's (CRU) monthly dataset at 0.5° resolution (Mitchell & Jones, 2005). We used the period 1961–2001 (Hirota et al., 2011) to obtain mean annual rainfall (MAR in mm/year), rainfall seasonality, and interannual rainfall variability. As measure of seasonality, we used Markham's Seasonality Index (MSI; Markham, 1970), which ranges from 0% to 100%. The index quantifies how evenly rainfall is distributed across the months in the year and thus captures both the severity and duration of dry (wet) periods in wet (dry) regions. As measure of interannual variability, we used the percentage of severely dry or wet years; a severely dry year is defined as $<-1.5\sigma$ and a severely wet year as $\geq 1.5\sigma$ from the mean annual rainfall (Holmgren et al., 2013). We obtained fire frequencies from the standard MODIS burned area product MCD45 Collection 5 (Roy, Boschetti, Justice, & Ju, 2008) for the years 2002–2010 which records for each cell on 500-m resolution whether it had burned in a given year. We took estimated densities of livestock as measured in tropical livestock units (TLU/km^2) from the Gridded Livestock of the World dataset (Robinson et al., 2014). We excluded all croplands, artificial surfaces, water, and bare ground, as defined as categories [11–30, 190–230] in the ESA 2009 Globcover dataset at 300-m resolution. We resampled all datasets to 250 m and took a regularly spaced sample with a distance of 0.1° (c. 10 km), which resulted in a dataset of c. 270,000 locations.

2.7 | Submodels

2.7.1 | Fire probabilities

In this submodel, we aimed to realistically capture the response of fire to changes in tree cover and rainfall conditions. Whether a

tropical location burns in a given year depends on the presence of an initial ignition source—whether natural or anthropogenic—and the flammability of the respective location. We assumed that the presence of an initial ignition source is independent of tree cover and rainfall. However, whether an ignition causes a cell to burn and whether this fire spreads to neighboring cells does depend on tree cover and rainfall. Together, fire ignition rate and the probabilities of its spread generate emergent fire frequencies that can be calibrated on remotely sensed fire data. Because the model is designed such that a cell can burn only once each year, to parameterize it we took the empirical probabilities of a location burning per year. We organized the empirical fire probabilities in bins of tree cover (bin width 2%) and annual rainfall (bin width 100 mm/year). The fire probability-tree cover relation $prob_F(T)$ (per year) follows a double Hill function (Van Nes et al., 2018):

$$prob_F(T) = p_1 \frac{T^{p_3}}{T^{p_3} + p_2^{p_3}} \frac{p_4^{p_5}}{p_4^{p_5} + T^{p_5}} \quad (2)$$

The fire probability-rainfall relation is hump-shaped (Dantas et al., 2016). We fitted a scaled logistic regression and Gaussian function to the fire-rainfall relation $prob_F(R)$ and found that the Gaussian was the most parsimonious one (as determined by the lowest value for the Akaike information criterion):

$$prob_F(R) = \exp^{-(R-p_6)^2/(2p_7^2)} \quad (3)$$

We combined the effects of tree cover (T; %) and annual rainfall (R; mm/year) into one equation for fire probability $prob_F(T, R)$ (per year):

$$prob_F(T, R) = p_1 \frac{T^{p_3}}{T^{p_3} + p_2^{p_3}} \frac{p_4^{p_5}}{p_4^{p_5} + T^{p_5}} \exp^{-(R-p_6)^2/(2p_7^2)} \quad (4)$$

We also explored how the empirical parameters in Equation 4 depend on rainfall variability V; we separately assessed the effects of seasonality S and interannual rainfall variability I in this equation.

We determined which parameter in Equation 4 is most sensitive to an increase in seasonality S in the following way. First, we established two subdatasets, one with all data points with average values of MSI (between 33rd and 67th percentiles, which are MSI values of 37% and 57%) and one with all data points one standard deviation above the average (between 67th and 97th percentiles, which are MSI values of 57% and 82%). We then separately fitted each of the parameters in the fire function on each of these datasets while keeping the remainder of the fire function intact. We compared the AIC values of the fits for the average and high MSI values. The parameter with largest absolute ΔAIC best explains the difference in fire frequency between average and high MSI. We found that this parameter is p_7, which describes the width of the Gaussian function of rainfall. We used the two estimates of p_7, for average and high MSI, to obtain a coefficient of variation of this parameter, CV_S, that captures the response of fire probability to deviations in seasonality (S) from its average (MSI in the range 37%–57%, or simply 47%); p_7 is replaced by $p_7 \, CV_S \frac{S}{47}$:

$$prob_F(T, R, S) = p_1 \frac{T^{p_3}}{T^{p_3} + p_2^{p_3}} \frac{p_4^{p_5}}{p_4^{p_5} + T^{p_5}} \exp^{-(R-p_6)^2/(2(p_7 \, CV_S \frac{S}{47})^2)} \quad (5)$$

We similarly explored the effects of interannual rainfall variability on fire probability. Both the standard deviation and coefficient of variation (CV) of annual rainfall were poor measures to detect general patterns in response to interannual variability because both are confounded by annual rainfall. However, we found that the percentage of severely dry or wet years affected fire probability consistently, where a severely dry year is defined as $<-1.5\sigma$ and a severely wet year as $\geq 1.5\sigma$ from the mean annual rainfall. As average interannual variability, we took a frequency of 5%–6% of either severely dry or wet years (30th–81st percentiles) and as one standard deviation higher than average we took 7%–8% (81st–99th percentiles). Here, we found that fitting the parameter that scales the fire function, p_1, gave a greater improvement in the fit than p_7. Thus, analogous to those for seasonality, we used the two estimates for the effects of interannual variability to obtain a coefficient of variation of p_1, CV_I, that captures the response of fire probability to deviations in interannual rainfall variability from its average (a frequency of severely dry/wet years (FSY) of 5%–6%, or simply 6%); p_1 is replaced by $p_1 CV_I \frac{FSY}{6}$:

$$prob_F(T, R, I) = p_1 CV_I \frac{FSY}{6} \frac{T^{p_3}}{T^{p_3} + p_2^{p_3}} \frac{p_4^{p_5}}{p_4^{p_5} + T^{p_5}} \exp^{-(R-p_6)^2/(2p_7^2)} \quad (6)$$

2.7.2 | Fire ignition and spread

The probability of a cell catching fire "spontaneously" (i.e., excluding fire spread from a neighboring cell) in a given year is the product of $prob_F$ and ignition rate p_{ign} (per year). We simulated in our lattice the emergent fire frequencies for different ignition rates and tree-cover values. We calculated the ignition rate that best fitted (least squared residuals) the empirical fire-tree cover relation for the rainfall level at which fire spread is at its maximum (p_6), because this is when ignition rate is most limiting for fire occurrence. We used this fitted ignition rate throughout our simulations. We performed the simulations assuming that fire spreads more easily than it ignites, which is reasonable for the dry-season fires that dominate the tropics (Archibald, Staver, & Levin, 2012). Because the parameter that scales the fire probability function is p_1, fire probability for cell i, j in case any of its eight neighbors is burning was set to $prob_F/p_1$. For rainfall, at peak fire frequency, this yielded a very high goodness of fit of fire frequency as a function of tree cover with $R^2 = 0.95$.

2.7.3 | Fire-induced tree-cover loss

In case a cell burns during a certain time step, its tree cover is reduced by a tree-cover-dependent loss function. This loss of tree cover after a fire was determined for each burnt cell in our dataset by subtracting tree cover in the year after a burn from tree cover in the year before the burn. For each tree-cover value T, we took the observed median per-capita fire-induced tree-cover loss and we subsequently fitted a third-degree polynomial to these medians. Thus,

fire-induced tree-cover loss becomes as follows (which does not allow for negative loss of tree cover):

$$F_{i,j}(T)(t) = \begin{cases} \max\left(0, a_3 T_{i,j}^3(t) + a_2 T_{i,j}^2(t) + a_1 T_{i,j}(t) + a_0\right) T_{i,j}(t) & \text{if } T_{i,j} \text{ burns} \\ 0 & \text{if } T_{i,j} \text{ does not burn} \end{cases}$$

$$(7)$$

where a_0, a_1, a_2, and a_3 are empirically obtained constants. We tested whether the results were caused by other factors than fire by repeating our analysis on unburned locations and did not find similar patterns (median tree-cover loss over a 2-year period was generally 0; see Supporting Information Figures S1 and S2).

2.7.4 | Tree-cover growth

Growth of tree cover in each cell ($T_{i,j}$ in %) is modeled as logistic growth (Waring, Newman, & Bell, 1981) with growth rate r (per year) with herbivore control $H(MAR, T)$ (per year) toward carrying capacity $K(MAR)$ (%):

$$G_{i,j}(MAR, T, H) = \max(0, r - H(MAR, T)) T_{i,j}(t) \left(1 - \frac{T_{i,j}(t)}{K(MAR)}\right) \quad (8)$$

Because maximum tree cover depends on MAR (Hirota et al., 2011; Sankaran et al., 2005), we estimated for bins of MAR (of width 100 mm/year) the carrying capacity of tree cover as the 99th percentile of tree cover. We fitted a Hill function to these results, which yielded the empirical carrying capacity $K(MAR)$:

$$K(MAR) = K_{max} \frac{MAR^n}{h_{MAR}^n + MAR^n} \quad (9)$$

where K_{max} (%) is the maximum tree-cover value in the data; h_{MAR} (mm/year) represents the value of MAR at which half the maximum carrying capacity is reached; and n (–) is an exponent.

We calculated the tree-cover growth rate r (per year) using time series of annual tree-cover data to determine for each burnt cell, the growth rate after a fire has occurred ($n = 60,724$ burns with subsequent unburned tree-cover recovery) (Flores et al., 2017) where we assumed logistic growth toward carrying capacity $K(MAR)$ (Waring et al., 1981). We thus obtained a location-specific growth rate, but although the tree-cover product that we use has already been successfully used to compute postfire recovery (Flores et al., 2017), it contains considerable uncertainties, resulting in high variation in estimates of growth rates. Therefore, we took the median growth rate in the dataset as growth rate r (per year) in the logistic growth function.

2.7.5 | Herbivory

Livestock densities (Robinson et al., 2014), measured in tropical livestock units (TLU/km²), can be considered as proxies for total herbivore pressure on tree juveniles. This is important, because global estimates of wild herbivore densities are lacking. Indeed, analysis of livestock densities and wild browser density estimates in Africa show a similar pattern across rainfall levels as livestock densities do

(Hempson et al., 2015). Herbivore pressure H (per year) is modeled as a control on growth rate and is the product of a loss coefficient m_H ($\%^{-1}$ TLU^{-1} km²) and herbivore density $dens_H$ (TLU/km²), which depends on MAR and tree cover:

$$H(MAR, T) = m_H \, dens_H(MAR, T) \quad (10)$$

where herbivore density $dens_H$ as a function of MAR and tree cover has the same structure as that for fire probability (see "Fire probabilities"):

$$dens_H(MAR, T) = l_1 \frac{T^{l_3}}{T^{l_3} + l_2^{l_3}} \frac{l_4^{l_5}}{l_4^{l_5} + T^{l_5}} e^{-(MAR-l)^2/(2l_7^2)} \quad (11)$$

m_H represents the effect of one tropical livestock unit (TLU/km²) on tree-cover growth rate. Data on this are lacking, but we used the estimated relation between dry matter consumption of herbivores, DMC_H, and that of fire, DMC_F, in Africa (Archibald & Hempson, 2016) as a proxy:

$$\frac{DMC_H}{DMC_F} = \exp^{0.84 - 0.00050 \, MAR} \quad (12)$$

Here, we assume that the ratio between dry matter consumed by herbivores and dry matter consumed by fire (Equation 12) is equivalent to the ratio between the effects of herbivores and fire on young trees, that is, that $\frac{DMC_H}{DMC_F} = \frac{m_H \cdot dens_H}{prob_F \cdot mort_{F,mean}}$. This yields the following equation for m_H at given MAR, $m_{H,MAR}$:

$$m_{H,MAR} = \frac{\exp^{0.84 - 0.00050 \, MAR} \cdot prob_{F,MAR} \cdot loss_{F,mean}}{dens_{H,MAR}} \quad (13)$$

To be on the conservative side, we took the ratio at the rainfall level at which herbivore density is at its peak (710 mm/year), so $m_H = m_{H,710}$.

We calculated the mean densities of the various species (in heads and TLU/km²) of each species in the livestock dataset (Robinson et al., 2014).

The dataset was assembled using ArcGIS, and subsequent analyses were carried out in MATLAB. All simulations were performed in GRIND for MATLAB. All parameters and their values are given in Table 1.

3 | RESULTS

Our parameterized model (Figures 1 and 2; Table 1) generates alternative stable states in tree cover with accompanying hysteresis against changing rainfall conditions (Figure 3, Supporting Information Figure S7). The underlying mechanisms are the feedback loops between tree cover and herbivory, and between tree cover and fire. At low tree-cover and rainfall levels, herbivory is the main mechanism that can maintain low tree cover, with herbivore density peaking at ~10% tree cover and 700 mm/year rainfall (Figure 1e,f). The feedback between tree cover and herbivory can maintain low tree cover up until 1,100 mm/year rainfall (Supporting Information Figure S8), a result that is robust against a wide range of parameter values in the herbivory-controlled growth term (Supporting Information

TABLE 1 The parameters and variables with their descriptions and values, and corresponding figure or reference

Symbol	Description	Value	Unit	Source
a_0	Constant in polynomial for fire-induced tree cover loss	−0.27	–	Figure 1c
a_1	Coefficient of first-degree term in polynomial for fire-induced tree cover loss	0.037	$\%^{-1}$	Figure 1c
a_2	Coefficient of second-degree term in polynomial for fire-induced tree cover loss	-9.1×10^{-4}	$\%^{-2}$	Figure 1c
a_3	Coefficient of second-degree term in polynomial for fire-induced tree cover loss	-7.2×10^{-6}	$\%^{-3}$	Figure 1c
CV_I	Coefficient of variation of p_1 for interannual rainfall variability	0.052	–	Not shown
CV_S	Coefficient of variation of p_7 for rainfall seasonality	0.32	–	Figure 2
$dens_H$	Livestock density as proxy for total herbivore pressure	$[0-l_1]$	TLU/km^2	Figure 1e–f
h_{MAR}	Half-saturation constant where carrying capacity is half its maximum	520	mm/year	Figure 1d
K_{max}	Maximum carrying capacity of tree cover	85	%	Figure 1d
l_1	Maximum livestock density	16	TLU/km^2	Figure 1e–f
l_2	Tree cover where livestock density rises sharpest	2.3	%	Figure 1e
l_3	Exponent in Hill function for rise in livestock density	3.6	–	Figure 1e
l_4	Tree cover where livestock density declines sharpest	21	%	Figure 1e
l_5	Exponent in Hill function for decline in livestock density	3.2	–	Figure 1e
l_6	Rainfall at which livestock density peaks	710	mm/year	Figure 1f
l_7	Standard deviation of Gaussian function of rainfall for livestock density	220	mm/year	Figure 1f
m_H	Herbivore-induced loss coefficient	8.0×10^{-3}	$\%^{-1}$ TLU^{-1} km^2	Archibald and Hempson (2016)
n	Exponent in Hill function for carrying capacity	2.7	–	Figure 1d
p_1	Maximum probability of catching fire upon ignition	0.31	per year	Figures 1a–b and 2
p_2	Tree cover where fire probability rises sharpest	1.6	%	Figures 1a and 2
p_3	Exponent in Hill function for rise in fire probability	1.7	–	Figures 1a and 2
p_4	Tree cover where fire probability declines sharpest	37	%	Figures 1a and 2
p_5	Exponent in Hill function for decline in fire probability	4.7	–	Figures 1a and 2
p_6	Rainfall at which fire probability peaks	1,100	mm/year	Figures 1b and 2
p_7	Standard deviation in Gaussian function of rainfall for fire probability	380	mm/year	Figures 1b and 2
p_{ign}	Probability of fire ignition in each cell	1.2×10^{-4}	per year	Supporting Information Figure S6
R	Rainfall	[0–2,000]	mm/year	N.A.
r	Growth rate of tree cover	0.016	per year	Not shown
T	Tree cover	$[0-K_{max}]$	%	N.A.
t	Time	[0–1,000]	year	N.A.

Figure S9). At intermediate rainfall levels, fire is the main mechanism that can maintain low tree cover. Fire probability peaks at low tree cover (around 10%–20%; Figure 1a) and at intermediate rainfall (around 1,100 mm/year; Figure 1b) across continents (Supporting Information Figure S3). Tree-cover loss by fire in such environments is around 20% of the originally present tree cover (Figure 1c; see Supporting Information Figure S1 for continental differences). Recovery from fire is then generally too slow to reach a closed canopy at the observed fire probabilities. When the model is initialized at observed climatic and tree-cover conditions, low tree cover often persists up to about 1,700 mm/year (Figure 3a). At high tree cover, fire probability is always low (Figure 2), which keeps it stable in the absence of further perturbations. The model predictions of stabilized tree cover correspond well with observed tree cover distributions, with $R^2 = 0.79$ for a linear regression.

Increasing seasonality of rainfall increases the width of the bell-shaped response of fire frequency to rainfall (Figure 1b) with 32% for one standard deviation of seasonality (Figure 2). This means that fire frequency peaks at a wider range of mean rainfall levels, implying a qualitative change in the relation between fire and rainfall. Increasing interannual variability of rainfall increases the height of the peak fire frequency with about 5% for one standard deviation of the frequency of severely dry or wet years (Supporting Information Figure S5; Table 1). Thus, despite a quantitative change, the relation between fire and rainfall remains the same with interannual variability. We find that this difference between seasonality and interannual

variability is reflected in how they affect the stability of tree cover in fire-prone areas: Interannual variability does not increase forest-savanna hysteresis, whereas seasonality does (Supporting Information Figure S7). Seasonality strongly increases the range of rainfall conditions where fire frequency is high: When seasonality is two standard deviations above its average, the low tree-cover state persists up to about 2,000 mm/year (Supporting Information Figure S7).

The stability of low tree cover depends on whether or not fire-spread probability is sufficiently high to allow for percolating fires, which appears to be largely determined by tree cover. Indeed, such fires would not propagate indefinitely (or during the whole fire season). They could be constrained by other landscape features (Hantson et al., 2017; Pueyo et al., 2010), unrelated to tree cover. However, we would expect noticeable increases in fire probability below the critical threshold at which trees impede percolation. We find high burned area in savannas up to c. 40% tree cover, indicating that such covers are clearly below the threshold (Supporting Information Figures S10 and S11). Under average seasonality, this is the case for rainfall ranges between c. 500 and 1,600 mm/year, which is the same range where fire-maintained low tree cover is predicted (Figures 3, Supporting Information Figure S7). With increasing seasonality, rainfall ceased to be a limiting factor (either too high or too low) and fire regimes became independent of mean annual rainfall levels (Supporting Information Figures S11 and S12). For tree cover above c. 40%, we do not find an increase in burned area with seasonality, indicating that fires cannot percolate forests even with large increases in seasonality (Supporting Information Figures S10 and S12).

We find nonlinear responses of both high and low tree cover to spatial perturbations: For relatively small clustered perturbations, the system recovers fully, but when a critical size is exceeded, a transition to the alternative state may occur. Figure 4 shows the results for perturbations to the high tree-cover state (see Supporting Information Figure S13 for similar results for the low tree-cover state). Beyond a critical perturbation size, the probability that fire ignites anywhere within that area can become so high that the perturbed cells no longer recover and the remaining high tree-cover cells are lost as well. Whether recovery occurs depends positively on average rainfall (Figure 4a). At average seasonality and 1,700 mm/year, tree cover recovers fully even after the largest possible perturbation (i.e., full loss of high tree cover); at 1,600 mm/year, it also generally grows back after 1,000 years; at 1,500 mm/year, recovery starts to depend on the size of the perturbation: With 30%–70% of the cells removed of their closed tree cover, the resulting landscape after 1,000 years consists of patches of both high and low tree cover. Above 70% removal, no high tree-cover cells are present after 1,000 years, so a tipping point has been crossed. A similar response is observed when seasonality is increased. Whereas the high tree cover state is fully resilient at 1,700 mm/year at average seasonality, tipping points may be crossed at higher seasonality: High tree-cover recovery does not always occur, and the critical perturbation level decreases with seasonality. For a range of perturbation sizes, high and low tree cover coexist after 1,000 years (Figure 4c).

There are differences in resilience to randomly distributed perturbations and clustered perturbations. After a run of 1,000 years, the response of the high tree-cover state to perturbations is more gradual in the clustered case than in the random case. In response to random perturbations, there is a clear threshold in the perturbation size above which a full loss of high tree cover occurs, but below which recovery rapidly occurs (Figure 4b,d). In response to clustered perturbations, we find a range of perturbation sizes after which both high and low tree-cover patches remain present even after 1,000 simulated years; after 5,000 years, however, the remaining patches with high tree cover will have disappeared (Supporting Information Figure S14).

4 | DISCUSSION

We quantified the full feedback between fire and tree cover and showed that it may generate alternative stable states of tree cover across rainfall levels in the tropics. Assessing the strength of the fire–tree cover feedback globally finally integrates pieces of evidence, ranging in scale from field studies (e.g., Dantas, Batalha, & Pausas, 2013) to pantropical remote sensing analyses (e.g., Hirota et al., 2011; Staver et al., 2011; Xu et al., 2016), that forests and savannas can be alternative stable states separated by tipping points. Although forests and savannas are defined by structure and species composition (Ratnam et al., 2011; Veldman, 2016), tree cover is a key aspect in their self-stabilizing dynamics.

We found an important effect of rainfall variability on fire-driven alternative stable states. It is known that in wet areas on the one hand, occasional dry periods enhance fire-prone conditions; in dry areas on the other hand, occasional wet periods stimulate fuel build-up for fires in dry periods (Archibald, Nickless, Govender, Scholes, & Lehsten, 2010; Archibald, Roy, van Wilgen, & Scholes, 2009; Bucini, Beckage, & Gross, 2017; Van der Werf, Randerson, Giglio, Gobron, & Dolman, 2008). However, we found that seasonal and interannual rainfall variability affect fire regimes in different ways with contrasting implications for forest-savanna stability. While a previous empirical analysis showed that tree cover in the wet tropics decreases with higher seasonality and interannual rainfall variability (Holmgren et al., 2013), our results suggest that it is mostly the intraannual seasonality that decreases forest resilience by promoting the savanna-stabilizing fire feedback.

Whereas in relatively wet savannas, low tree cover can be explained by frequent fires, and in drier savannas, tree cover is often below carrying capacity (Sankaran et al., 2005). In drier savannas, herbivory of young tree seedlings and saplings can suppress tree cover (Staver & Bond, 2014), creating a herbivory–vegetation feedback comparable to the fire–vegetation feedback (Dantas et al., 2016; Van Langevelde et al., 2003). To account for herbivory, we included livestock densities as a proxy of global herbivore densities (Archibald & Hempson, 2016; Hempson et al., 2015; Robinson et al., 2014). These estimates suggest that herbivores could greatly suppress tree cover up to 1,100 mm/year rainfall even in the absence of fire.
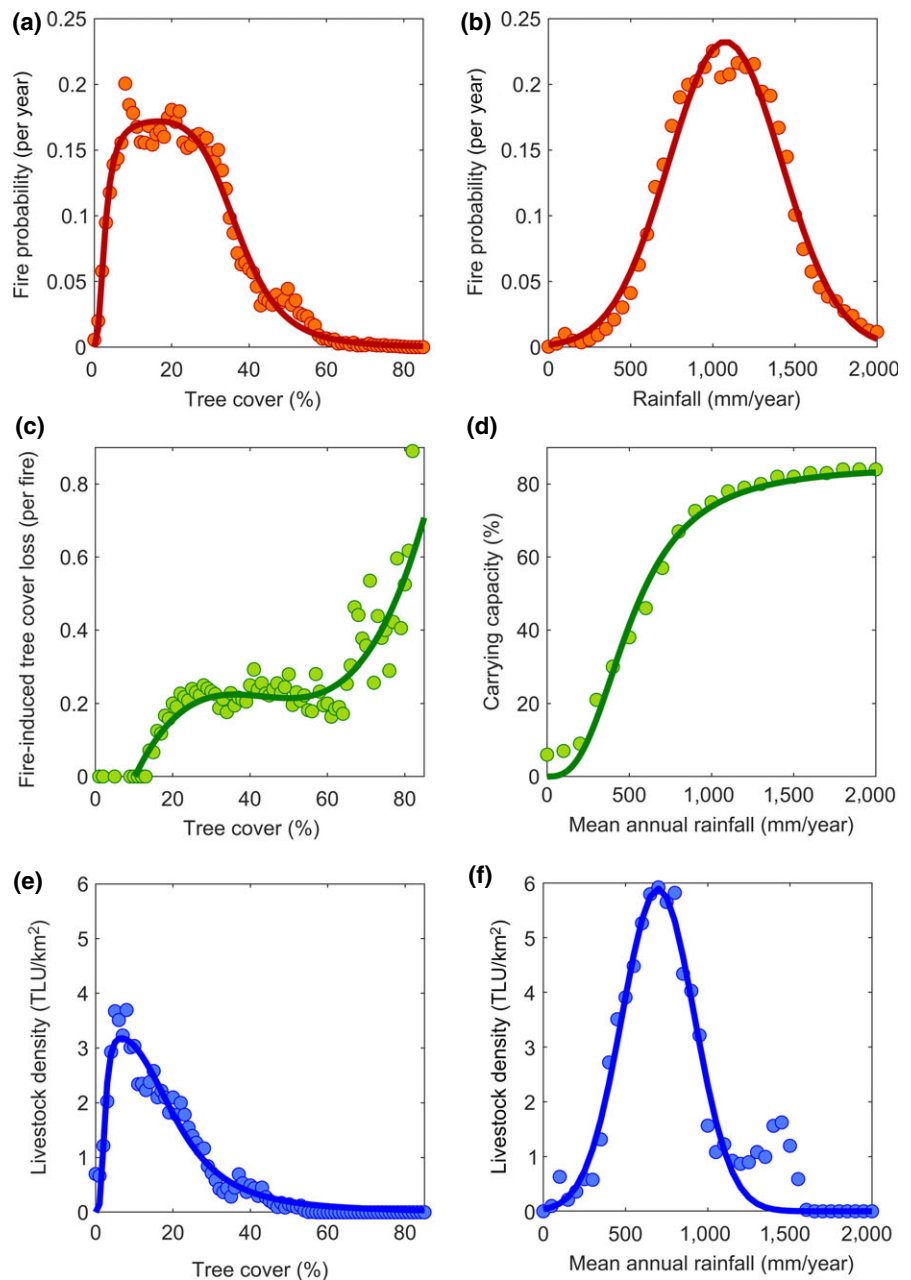
FIGURE 1 Parameterizations of the model as functions of tree cover and rainfall across the tropics. (a) Mean fire probability (per year) as a function of tree cover (%). (b) Mean fire probability (per year) as a function of rainfall in the fire year (mm/year). (c) Median fire-induced per-capita tree cover loss (per fire) as a function of tree cover (%). (d) Carrying capacity for tree cover (%) as a function of mean annual rainfall (mm/year). (e) Livestock density (tropical livestock units/km^2; TLU/km^2) as a function of tree cover (%). (f) Livestock density (TLU/km^2) as a function of mean annual rainfall. Livestock density is used as a proxy for herbivore pressure on tree cover

There are similarities and differences between the herbivore–tree cover feedback and fire–tree cover feedback. Both herbivores and fires are more abundant in open landscapes with lower tree cover, and they both have negative effects on tree cover that contribute to maintaining these open landscapes. Indeed, both fires and herbivores show a steep increase in abundance below a critical tree cover (Figure 1a,e). It is this shape that allows for the existence of alternative stable states under a range of assumed growth and loss curves for tree cover (Kitzberger, Aráoz, Gowda, Mermoz, & Morales, 2012; Van Nes et al., 2018; also see Supporting Information Figure S9). This parallel structure of the two feedbacks is worth highlighting, but it is important to also recognize their differences. Herbivores are more selective in their effect on tree cover than fire. This selectivity is probably reflected in the herbivore–tree cover feedback acting at lower rainfall levels because herbivores are unable to control fast

plant growth with a higher proportion of unpalatable tissue at higher rainfall levels. Fires, in contrast, can exert a bottom-up control on tree cover at higher rainfall levels. Also, whereas the fire–tree cover feedback responds strongly to rainfall seasonality, mammalian herbivory is relatively insensitive to seasonality (Archibald & Hempson, 2016). Interestingly, field experimental evidence shows that in dry environments, interannual pulses of rainfall may allow windows of opportunity for trees to escape herbivory and increase tree cover (Holmgren, Lopez, Gutierrez, & Squeo, 2006; Holmgren et al., 2013; Sitters, Holmgren, Stoorvogel, & López, 2012). The contrasting response of the herbivore–tree cover feedback to seasonal vs. inter-annual rainfall variability may be explained by the predictability of the rainfall events. Trees can escape herbivore control when their growth as a response to the rainfall pulse is faster than the herbi-vore response to the increase in primary productivity (Scheffer, van
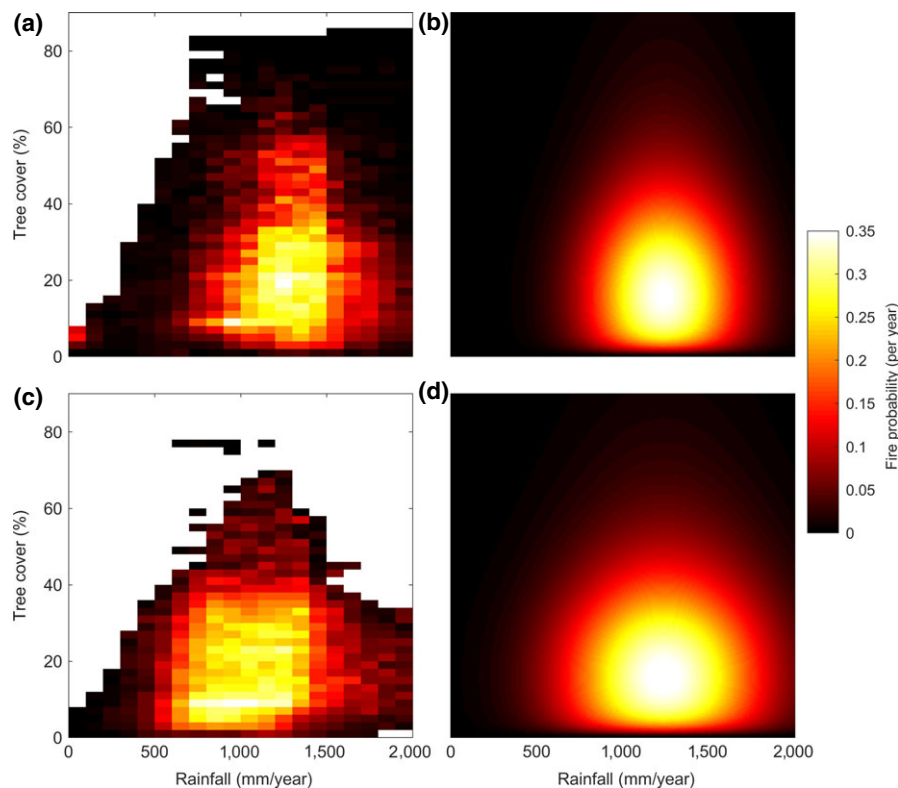
FIGURE 2 Observations and fits of the effects of rainfall on fire probabilities across the tropics. (a) Observed and (b) fitted mean fire probability (per year) as a function of annual rainfall (mm/year) and tree cover (%) for average rainfall seasonality. (c) Observed and (d) fitted mean fire probability (per year) as a function of annual rainfall (mm/year) and tree cover (%) for rainfall seasonality one standard deviation above average. The greatest improvement in fitting the data in (c) was obtained by adjusting the standard deviation of the Gaussian function of rainfall (also see Figure 1b, Methods), meaning that primarily the range of annual rainfall levels at which fire probability is high expands with rainfall seasonality. See Supporting Information Figure S4 for an extrapolation of these fits to higher levels of seasonality

Nes, Holmgren, & Hughes, 2008). This critical rate for trees to escape top-down control may be more likely to occur during an unpredictable interannual rainfall pulse. The fire and herbivore feedbacks with tree cover also interact. The fact that both fires and browsing negatively affect tree cover creates a synergy between both feedbacks (Van Langevelde et al., 2003). However, fires and grazing also interact via grass biomass. Grasses act as both fuel for fires and food for grazers, making them competitors for the same resource (Bond & Keeley, 2005). Thus, grazing and fire can impede one another, such that grazing may result in woody encroachment through fire suppression (Roques, O'Connor, & Watkinson, 2001).

Anthropogenic or natural disturbances may locally alter tree cover and thereby fire probability. Moreover, the size of a spatial disturbance may affect subsequent recovery (Van de Leemput, Dakos, Scheffer, & van Nes, 2018). We therefore performed perturbation experiments in which our simulated high tree cover (and low tree cover) landscapes are subject to perturbations of varying size. To this end, we differentiated between clustered perturbations, in which a "deforestation" (and "afforestation") of a single square area is imposed, and randomly distributed perturbations. We showed that both types of perturbation to the high tree cover state (low tree cover state) may cross a tipping point (sensu Van Nes et al., 2016), meaning that the entire lattice undergoes a transition. However, the

transition in response to a clustered perturbation takes longer than to a random perturbation, whereas the clustered perturbation requires a smaller critical size. From this follows that the question to which type of perturbation the ecosystem is most resilient becomes a matter of time scale: Although a tipping point is more easily crossed when the perturbation is more clustered, it is also slower, which may provide more opportunity to respond and conserve the system. In either case, whether or not such a tipping point can be crossed depends on the average rainfall and its seasonality. Still, it should be noted that the mechanism of disturbance itself plays an important role, too. For example, deforestation by humans is often accompanied by fires (Aragão et al., 2008), whereas a natural disturbance such as a hurricane may not. Also, we assume that tree cover is tightly linked to grass cover, which is not necessarily true, for instance in case of selective logging (Veldman, Mostacedo, Peña-Claros, & Putz, 2009).

We found that the effect of fire on tree cover clearly differs between savannas and forests. In savannas with tree cover between 20% and 60%, a single fire typically clears about 20% of the tree cover that is present. When tree cover is above 60%, however, the effect of fire is much higher. We found that the per-capita loss of tree cover in these landscapes lies around 60% or three times as high as in savannas. These numbers agree with mortality rates
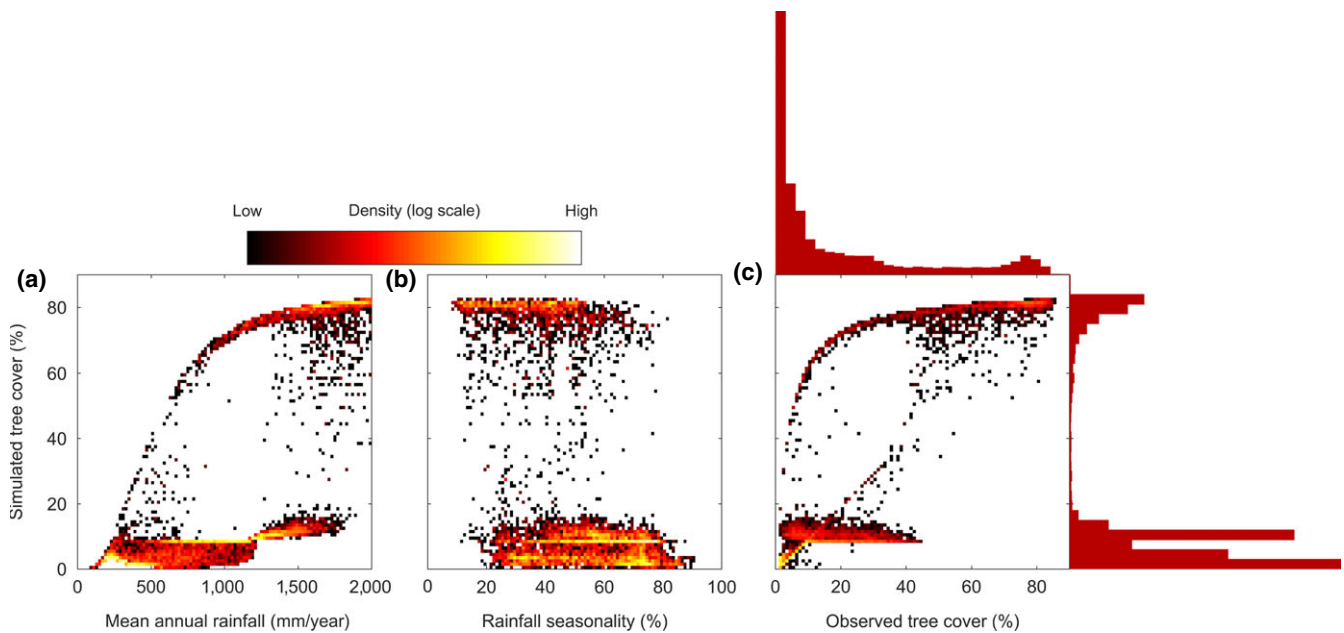
FIGURE 3 Densities of simulated tree cover (%) against (a) mean annual rainfall (mm/year), (b) rainfall seasonality (%) and (c) observed tree cover (%). All plots show results of 10,000 simulations in which the model was initialized with one randomly selected location with the observed tree cover, mean annual rainfall, and rainfall seasonality. Simulations were performed for 1,000 years. Roughly between 500 and 1,700 mm/year rainfall (see a) and between 20% and 80% seasonality (see b), a tree cover state below carrying capacity is predicted to be possible. The histograms in (c) show multimodal patterns of both observed and simulated tree cover, which indicate alternative stable states. The low density of tree cover values just below 10% in the simulated results is explained by the absence of effect of fire below this value (see Figure 1c)

observed in the field (Hoffmann et al., 2009). Closed tree canopies are generally dominated by forest-tree species (Ratnam et al., 2011), which, as opposed to those in savannas, have not evolved in conditions with regular fires (Keeley, Pausas, Rundel, Bond, & Bradstock, 2011). Apart from differences between ecosystem types, there are differences among continents in ecosystem structure (Xu et al., 2018) and in fire ecology (Lehmann et al., 2014). For example, fire frequency is relatively high in Africa (Giglio, Randerson, & van der Werf, 2013; Van Nes et al., 2018), although that may be counteracted by relatively low fire intensity (Dantas & Pausas, 2013) and relatively high recovery from disturbances in that continent (Schwalm et al., 2017).

Our model resembles an early spatial forest-fire model including fuel build-up and fires spreading through the lattice (Bak, Chen, & Tang, 1990; Drossel & Schwabl, 1992). This model was further developed afterward by including weather-dependent fires and gradual fuel succession (Pueyo, 2007; Pueyo et al., 2010). We added several novelties to this line of work, including empirically derived tree-cover-dependent fire probabilities and tree-cover-dependent fire-induced losses of tree cover. These improvements to the model were parameterized based on remotely sensed data. Although our parameterized model can help to understand the tropical fire–vegetation feedback and its emergent effects such as bimodalities in tree cover (Accatino & De Michele, 2016; D'Odorico, Laio, & Ridolfi, 2006; De Michele & Accatino, 2014; Van Nes et al., 2018), a number of relevant factors remain to be explored in future work. Continental differences in fire dynamics (Hantson et al., 2017; Lehmann et al.,

2014) should be further disentangled to make the model more suitable for localized predictions. It could then be used to explore the joint effects of climatic and land-use changes on fire dynamics. We have shown that with increasing rainfall variability, fire sizes may increase and forests may lose their stability. Small increases in fire-spread probability may indeed cause sudden increases in fire size and burned area (Archibald et al., 2012; Pueyo et al., 2010). However, in recent years, fires have become smaller due to land-use changes (Andela et al., 2017; Hantson, Pueyo, & Chuvieco, 2015), partly because humans alter the connectivity of the landscape (Andela et al., 2017) or actively suppress fire (Durigan & Ratter, 2016). Given that the configuration of fire-prone areas determines whether or not the landscape tips toward a closed canopy or remains open, the effects of land-use changes could be highly nonlinear.

Our spatial model provides a framework in which these and other nonlinearities, caused by interactions among for instance rainfall conditions, land use (Andela et al., 2017), herbivory (Archibald & Hempson, 2016), and CO_2 fertilization (Higgins & Scheiter, 2012), could be studied. Because the model represents the scale of remote sensing data (250 m), it bridges a gap between observations and theory and therefore occupies a promising niche that could stimulate new insights in tropical fire-vegetation dynamics (see also Hébert-Dufresne et al., 2018). On the observational side, the work on remotely sensed tropical tree cover indicating alternative stable states has so far been mostly based on static patterns instead of dynamic ones (Hirota et al., 2011; Holmgren et al., 2013; Staal et al., 2016; Staver
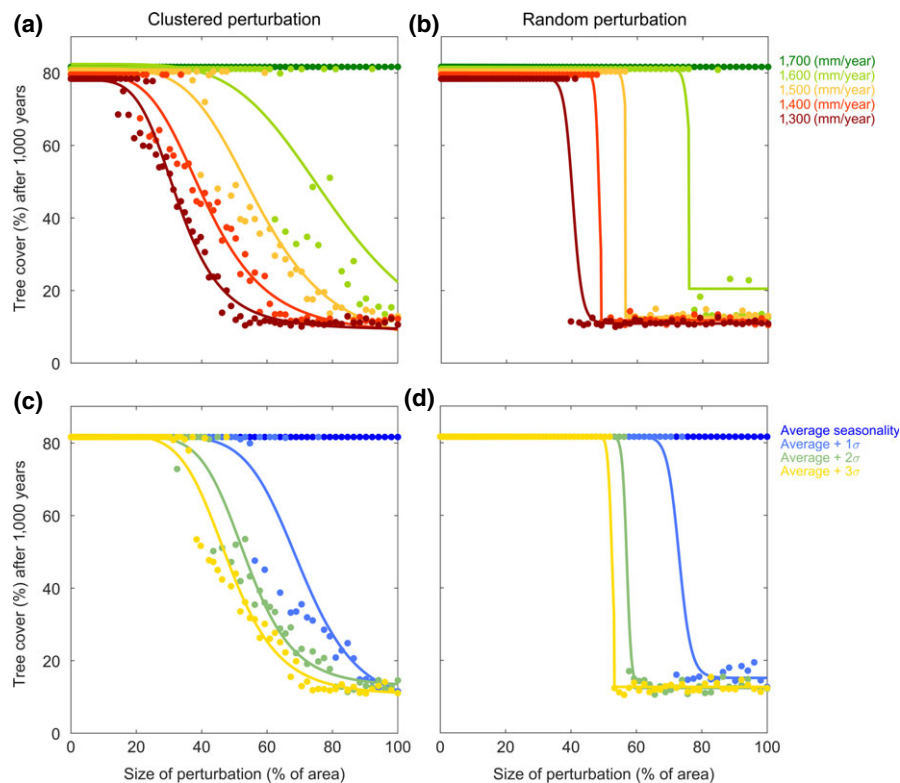
FIGURE 4 The effects of spatial perturbations to the high tree cover state of different size and configuration for different rainfall conditions. Perturbations were imposed by setting tree cover to 10%. (a) Tree cover after 1,000 years for different mean annual rainfall values (1,300–1,700 mm/year) at average rainfall variability, after a clustered perturbation of increasing size. (b) Tree cover after 1,000 years for different mean annual rainfall values (1,300–1,700 mm/year) at average rainfall variability, after a random perturbation of increasing size. (c) Tree cover after 1,000 years for different rainfall variabilities (0–3 standard deviations from the average) at 1,700 mm/year rainfall, after a clustered perturbation of increasing size. (d) Tree cover after 1,000 years for different rainfall variabilities (0–3 standard deviations from the average) at 1,700 mm/year rainfall, after a random perturbation of increasing size

et al., 2011; e.g., Bucini et al., 2017; but see Wuyts, Champneys, & House, 2017), which hampers the inference of temporal dynamics. On the theoretical side, models have considered spatial interactions between trees and fire (e.g., Accatino & De Michele, 2016; Archibald et al., 2012; Bacelar, Calabrese, & Hernández-García, 2014; Beckage, Gross, & Platt, 2011; Favier, Chave, Fabing, Schwartz, & Dubois, 2004; Hébert-Dufresne et al., 2018; Hochberg, Menaut, & Gignoux, 1994; Menaut, Gignoux, Prado, & Clobert, 1990; Schertzer et al., 2015; Wuyts et al., 2017), and nonspatial models have aimed to capture tree-cover patterns at the spatial scale of remote sensing data (e.g., Accatino & De Michele, 2013; Staal, Dekker, Hirota, & van Nes, 2015; Staver & Levin, 2012; Van Nes et al., 2014, 2018). However, these lack the remote sensing-based full quantification of the fire–tree cover feedback and its spatial implementation that we do provide. It is important to account for spatial fire dynamics, because such dynamics are essential for reflecting how fires affect the future probabilities and distribution of fires, which may be critical for the relative stability of forests and savannas (Archibald et al., 2012; Durrett & Levin, 1994; Pueyo, 2007; Schertzer et al., 2015). Ultimately, understanding these cross-scale complex dynamics is necessary for predicting how the structure of tropical landscapes, with implications for carbon storage and local livelihoods, may change in the future.

ORCID

Arie Staal iD http://orcid.org/0000-0001-5409-1436
Marten Scheffer iD http://orcid.org/0000-0002-2100-0312

REFERENCES

Accatino, F., & de Michele, C. (2013). Humid savanna–forest dynamics: A matrix model with vegetation–fire interactions and seasonality. *Ecological Modelling, 265,* 170–179.

Accatino, F., & de Michele, C. (2016). Interpreting woody cover data in tropical and subtropical areas: Comparison between the equilibrium and the non-equilibrium assumption. *Ecological Complexity*, 25, 60–67.

Andela, N., Morton, D. C., Giglio, L., Chen, Y., van der Werf, G. R., Kasibhatla, P. S., … Randerson, J. T. (2017). A human-driven decline in global burned area. *Science*, 356, 1356–1362.

Aragão, L. E. O. C., Malhi, Y., Barbier, N., Lima, A., Shimabukuro, Y., Anderson, L., & Saatchi, S. (2008). Interactions between rainfall, deforestation and fires during recent years in the Brazilian Amazonia. *Philosophical Transactions of the Royal Society of London. Series B, Biological Sciences*, 363, 1779–1785.

Archibald, S., & Hempson, G. P. (2016). Competing consumers: Contrasting the patterns and impacts of fire and mammalian herbivory in Africa. *Philosophical Transactions of the Royal Society of London. Series B, Biological Sciences*, 371, 20150309.

Archibald, S., Nickless, A., Govender, N., Scholes, R. J., & Lehsten, V. (2010). Climate and the inter-annual variability of fire in southern Africa: A meta-analysis using long-term field data and satellite-derived burnt area data. *Global Ecology and Biogeography*, 19, 794–809.

Archibald, S., Roy, D. P., van Wilgen, B. W., & Scholes, R. J. (2009). What limits fire? An examination of drivers of burnt area in Southern Africa. *Global Change Biology*, 15, 613–630.

Archibald, S., Staver, A. C., & Levin, S. A. (2012). Evolution of human-driven fire regimes in Africa. *Proceedings of the National Academy of Sciences of the United States of America*, 109, 847–852.

Bacelar, F. S., Calabrese, J. M., & Hernández-García, E. (2014). Exploring the tug of war between positive and negative interactions among savanna trees: Competition, dispersal, and protection from fire. *Ecological Complexity*, 17, 140–148.

Bak, P., Chen, K., & Tang, C. (1990). A forest-fire model and some thoughts on turbulence. *Physics Letters A*, 147, 297–300.

Bathiany, S., Dakos, V., Scheffer, M., & Lenton, T. M. (2018). Climate models predict increasing temperature variability in poor countries. *Science Advances*, 4, eaar5809.

Beckage, B., Gross, L. J., & Platt, W. J. (2011). Grass feedbacks on fire stabilize savannas. *Ecological Modelling*, 222, 2227–2233.

Boisier, J. P., Ciais, P., Ducharne, A., & Guimberteau, M. (2015). Projected strengthening of Amazonian dry season by constrained climate model simulations. *Nature Climate Change*, 5, 656–660.

Bond, W. J., & Keeley, J. E. (2005). Fire as a global 'herbivore': The ecology and evolution of flammable ecosystems. *Trends in Ecology & Evolution*, 20, 387–394.

Bucini, G., Beckage, B., & Gross, L. J. (2017). Climate seasonality, fire and global patterns of tree cover. *Frontiers of Biogeography*, 9, e33610.

Dantas, Vd L, Batalha, M. A., & Pausas, J. G. (2013). Fire drives functional thresholds on the savanna-forest transition. *Ecology*, 94, 2454–2463.

Dantas, Vd L, Hirota, M., Oliveira, R. S., & Pausas, J. G. (2016). Disturbance maintains alternative biome states. *Ecology Letters*, 19, 12–19.

Dantas, Vd L, & Pausas, J. G. (2013). The lanky and the corky: Fire-escape strategies in savanna woody species. *Journal of Ecology*, 101, 1265–1272.

De Michele, C., & Accatino, F. (2014). Tree cover bimodality in savannas and forests emerging from the switching between two fire dynamics. *PLoS ONE*, 9, e91195.

DeAngelis, D. L., & Yurek, S. (2017). Spatially explicit modeling in ecology: A review. *Ecosystems*, 20, 284–300.

DiMiceli, C. M., Carroll, M. L., Sohlberg, R. A., Huang, C., Hansen, M. C., & Townshend, J. R. G. (2011). *Annual global automated MODIS vegetation continuous fields (MOD44B) at 250 m spatial resolution for data years beginning day 65, 2000–2010, collection 5 percent tree cover.* College Park, MD: University of Maryland.

D'Odorico, P., Laio, F., & Ridolfi, L. (2006). A probabilistic analysis of fire-induced tree-grass coexistence in savannas. *The American Naturalist*, 167, E79–E87.

D'Onofrio, D., von Hardenberg, J., & Baudena, M. (2018). Not only trees: Grasses determine African tropical biome distributions via water limitation and fire. *Global Ecology and Biogeography*, 27, 714–725.

Drossel, B., & Schwabl, F. (1992). Self-organized critical forest-fire model. *Physical Review Letters*, 69, 1629–1632.

Durigan, G., & Ratter, J. A. (2016). The need for a consistent fire policy for Cerrado conservation. *Journal of Applied Ecology*, 53, 11–15.

Durrett, R., & Levin, S. (1994). The importance of being discrete (and spatial). *Theoretical Population Biology*, 46, 363–394.

Favier, C., Chave, J., Fabing, A., Schwartz, D., & Dubois, M. A. (2004). Modelling forest-savanna mosaic dynamics in man-influenced environments: Effects of fire, climate and soil heterogeneity. *Ecological Modelling*, 171, 85–102.

Flores, B. M., Holmgren, M., Xu, C., van Nes, E. H., Jakovac, C. C., Mesquita, R. C. G., & Scheffer, M. (2017). Floodplains as an Achilles' heel of Amazonian forest resilience. *Proceedings of the National Academy of Sciences of the United States of America*, 114, 4442–4446.

Giglio, L., Randerson, J. T., & van der Werf, G. R. (2013). Analysis of daily, monthly, and annual burned area using the fourth-generation global fire emissions database (GFED4). *Journal of Geophysical Research: Biogeosciences*, 118, 317–328.

Grimm, V., Berger, U., Bastiansen, F., Eliassen, S., Ginot, V., Giske, J., … DeAngelis, D. L. (2006). A standard protocol for describing individual-based and agent-based models. *Ecological Modelling*, 198, 115–126.

Hantson, S., Arneth, A., Harrison, S. P., Kelley, D. I., Prentice, I. C., Rabin, S. S., … Yue, C. (2016). The status and challenge of global fire modelling. *Biogeosciences*, 13, 3359–3375.

Hantson, S., Pueyo, S., & Chuvieco, E. (2015). Global fire size distribution is driven by human impact and climate. *Global Ecology and Biogeography*, 24, 77–86.

Hantson, S., Scheffer, M., Pueyo, S., Xu, C., Lasslop, G., van Nes, E. H., … Mendelsohn, J. (2017). Rare, intense, big fires dominate the global tropics under drier conditions. *Scientific Reports*, 7, 14374.

Hébert-Dufresne, L., Pellegrini, A. F. A., Bhat, U., Redner, S., Pacala, S. W., & Berdahl, A. M. (2018). Edge fires drive the shape and stability of tropical forests. *Ecology Letters*, 21, 794–803.

Hempson, G. P., Archibald, S., & Bond, W. J. (2015). A continent-wide assessment of the form and intensity of large mammal herbivory in Africa. *Science*, 350, 1056–1061.

Higgins, S. I., & Scheiter, S. (2012). Atmospheric CO_2 forces abrupt vegetation shifts locally, but not globally. *Nature*, 488, 209–212.

Hirota, M., Holmgren, M., van Nes, E. H., & Scheffer, M. (2011). Global resilience of tropical forest and savanna to critical transitions. *Science*, 334, 232–235.

Hochberg, M. E., Menaut, J. C., & Gignoux, J. (1994). The influences of tree biology and fire in the spatial structure of the West African savannah. *Journal of Ecology*, 82, 217–226.

Hoffmann, W. A., Adasme, R., Haridasan, M., de Carvalho, M. T., Geiger, E. L., Pereira, M. A., … Franco, A. C. (2009). Tree topkill, not mortality, governs the dynamics of savanna-forest boundaries under frequent fire in central Brazil. *Ecology*, 90, 1326–1337.

Hoffmann, W. A., Geiger, E. L., Gotsch, S. G., Rossatto, D. R., Silva, L. C., Lau, O. L., … Franco, A. C. (2012). Ecological thresholds at the savanna-forest boundary: How plant traits, resources and fire govern the distribution of tropical biomes. *Ecology Letters*, 15, 759–768.

Holmgren, M., Hirota, M., van Nes, E. H., & Scheffer, M. (2013). Effects of interannual climate variability on tropical tree cover. *Nature Climate Change*, 3, 755–758.

Holmgren, M., Lopez, B. C., Gutierrez, J. R., & Squeo, F. A. (2006). Herbivory and plant growth rate determine the success of El Niño Southern Oscillation-driven tree establishment in semiarid South America. *Global Change Biology*, 12, 2263–2271.

Huang, P., Xie, S.-P., Hu, K., Huang, G., & Huang, R. (2013). Patterns of the seasonal response of tropical rainfall to global warming. *Nature Geoscience*, 6, 357–361.

Keeley, J. E., Pausas, J. G., Rundel, P. W., Bond, W. J., & Bradstock, R. A. (2011). Fire as an evolutionary pressure shaping plant traits. *Trends in Plant Science*, 16, 406–411.

Kitzberger, T., Aráoz, E., Gowda, J. H., Mermoz, M., & Morales, J. M. (2012). Decreases in fire spread probability with forest age promotes alternative community states, reduced resilience to climate variability and large fire regime shifts. *Ecosystems*, 15, 97–112.

Lasslop, G., Brovkin, V., Reick, C. H., Bathiany, S., & Kloster, S. (2016). Multiple stable states of tree cover in a global land surface model due to a fire-vegetation feedback. *Geophysical Research Letters*, 43, 6324–6331.

Lehmann, C. E., Anderson, T. M., Sankaran, M., Higgins, S. I., Archibald, S., Hoffmann, W. A., … Bond, W. J. (2014). Savanna vegetation-fire-climate relationships differ among continents. *Science*, 343, 548–552.

Markham, C. G. (1970). Seasonality of precipitation in the United States. *Annals of the Association of American Geographers*, 60, 593–597.

Menaut, J. C., Gignoux, J., Prado, C., & Clobert, J. (1990). Tree community dynamics in a humid savanna of the Cote-d'Ivoire: Modelling the effects of fire and competition with grass and neighbours. *Journal of Biogeography*, 17, 471–481.

Mitchell, T. D., & Jones, P. D. (2005). An improved method of constructing a database of monthly climate observations and associated high-resolution grids. *International Journal of Climatology*, 25, 693–712.

Murphy, B. P., & Bowman, D. M. J. S. (2012). What controls the distribution of tropical forest and savanna? *Ecology Letters*, 15, 748–758.

Oesterheld, M., Sala, O. E., & McNaughton, S. J. (1992). Effect of animal husbandry on herbivore-carrying capacity at a regional scale. *Nature*, 356, 234–236.

Pausas, J. G., & Dantas, Vd L (2017). Scale matters: Fire–vegetation feedbacks are needed to explain tropical tree cover at the local scale. *Global Ecology and Biogeography*, 26, 395–399.

Pueyo, S. (2007). Self-organised criticality and the response of wildland fires to climate change. *Climatic Change*, 82, 131–161.

Pueyo, S., de Alencastro Graça, P. M. L., Barbosa, R. I., Cots, R., Cardona, E., & Fearnside, P. M. (2010). Testing for criticality in ecosystem dynamics: The case of Amazonian rainforest and savanna fire. *Ecology Letters*, 13, 793–802.

Ratnam, J., Bond, W. J., Fensham, R. J., Hoffmann, W. A., Archibald, S., Lehmann, C. E. R., … Sankaran, M. (2011). When is a 'forest' a savanna, and why does it matter? *Global Ecology and Biogeography*, 20, 653–660.

Robinson, T. P., Wint, G. R., Conchedda, G., Van Boeckel, T. P., Ercoli, V., Palamara, E., … Gilbert, M. (2014). Mapping the global distribution of livestock. *PLoS ONE*, 9, e96084.

Roques, K. G., O'Connor, T. G., & Watkinson, A. R. (2001). Dynamics of shrub encroachment in an African savanna: Relative influences of fire, herbivory, rainfall and density dependence. *Journal of Applied Ecology*, 38, 268–280.

Roy, D. P., Boschetti, L., Justice, C. O., & Ju, J. (2008). The collection 5 MODIS burned area product—Global evaluation by comparison with the MODIS active fire product. *Remote Sensing of Environment*, 112, 3690–3707.

Sankaran, M., Hanan, N. P., Scholes, R. J., Ratnam, J., Augustine, D. J., Cade, B. S., … Zambatis, N. (2005). Determinants of woody cover in African savannas. *Nature*, 438, 846–849.

Sankaran, M., Ratnam, J., & Hanan, N. (2008). Woody cover in African savannas: The role of resources, fire and herbivory. *Global Ecology and Biogeography*, 17, 236–245.

Scheffer, M., Carpenter, S., Foley, J. A., Folke, C., & Walker, B. (2001). Catastrophic shifts in ecosystems. *Nature*, 413, 591–596.

Scheffer, M., van Nes, E. H., Holmgren, M., & Hughes, T. (2008). Pulse-driven loss of top-down control: The critical-rate hypothesis. *Ecosystems*, 11, 226–237.

Schertzer, E., Staver, A. C., & Levin, S. A. (2015). Implications of the spatial dynamics of fire spread for the bistability of savanna and forest. *Journal of Mathematical Biology*, 70, 329–341.

Schwalm, C. R., Anderegg, W. R. L., Michalak, A. M., Fisher, J. B., Biondi, F., Koch, G., … Tian, H. (2017). Global patterns of drought recovery. *Nature*, 548, 202–205.

Sitters, J., Holmgren, M., Stoorvogel, J. J., & López, B. C. (2012). Rainfall-tuned management facilitates dry forest recovery. *Restoration Ecology*, 20, 33–42.

Staal, A., Dekker, S. C., Hirota, M., & van Nes, E. H. (2015). Synergistic effects of drought and deforestation on the resilience of the southeastern Amazon rainforest. *Ecological Complexity*, 22, 65–75.

Staal, A., Dekker, S. C., Xu, C., & van Nes, E. H. (2016). Bistability, spatial interaction, and the distribution of tropical forests and savannas. *Ecosystems*, 19, 1080–1091.

Staal, A., Tuinenburg, O. A., Bosmans, J. H. C., Holmgren, M., van Nes, E. H., Scheffer, M., … Dekker, S. C. (2018). Forest-rainfall cascades buffer against drought across the Amazon. *Nature Climate Change*, 8, 539–543.

Staver, A. C., Archibald, S., & Levin, S. A. (2011). The global extent and determinants of savanna and forest as alternative biome states. *Science*, 334, 230–232.

Staver, A. C., & Bond, W. J. (2014). Is there a 'browse trap'? Dynamics of herbivore impacts on trees and grasses in an African savanna. *Journal of Ecology*, 102, 595–602.

Staver, A. C., & Levin, S. A. (2012). Integrating theoretical climate and fire effects on savanna and forest systems. *The American Naturalist*, 180, 211–224.

Van de Leemput, I. A., Dakos, V., Scheffer, M., & van Nes, E. H. (2018). Slow recovery from local disturbances as an indicator for loss of ecosystem resilience. *Ecosystems*, 21, 141–152.

Van der Werf, G. R., Randerson, J. T., Giglio, L., Gobron, N., & Dolman, A. J. (2008). Climate controls on the variability of fires in the tropics and subtropics. *Global Biogeochemical Cycles*, 22, GB3028.

Van Langevelde, F., van de Vijver, C. A. D. M., Kumar, L., van de Koppel, J., de Ridder, N., van Andel, J., … Rietkerk, M. (2003). Effects of fire and herbivory on the stability of savanna ecosystems. *Ecology*, 84, 337–350.

Van Nes, E. H., Arani, B. M. S., Staal, A., van der Bolt, B., Flores, B. M., Bathiany, S., & Scheffer, M. (2016). What do you mean, 'tipping point'? *Trends in Ecology & Evolution*, 31, 902–904.

Van Nes, E. H., Hirota, M., Holmgren, M., & Scheffer, M. (2014). Tipping points in tropical tree cover: Linking theory to data. *Global Change Biology*, 20, 1016–1021.

Van Nes, E. H., Staal, A., Hantson, S., Holmgren, M., Pueyo, S., Bernardi, R. E., … Scheffer, M. (2018). Fire forbids fifty-fifty forest. *PLoS ONE*, 18, e0191027.

Veldman, J. W. (2016). Clarifying the confusion: Old-growth savannahs and tropical ecosystem degradation. *Philosophical Transactions of the Royal Society of London. Series B, Biological Sciences*, 371, 20150306.

Veldman, J. W., Mostacedo, B., Peña-Claros, M., & Putz, F. E. (2009). Selective logging and fire as drivers of alien grass invasion in a Bolivian tropical dry forest. *Forest Ecology and Management*, 258, 1643–1649.

Waring, R. H., Newman, K., & Bell, J. (1981). Efficiency of tree crowns and stemwood production at different canopy leaf densities. *Forestry*, 54, 129–137.

Wuyts, B., Champneys, A. R., & House, J. I. (2017). Amazonian forest-savanna bistability and human impact. *Nature Communications*, 8, 15519.

Xu, C., Hantson, S., Holmgren, M., van Nes, E. H., Staal, A., & Scheffer, M. (2016). Remotely sensed canopy height reveals three pantropical ecosystem states. *Ecology*, 97, 2518–2521.

Xu, C., Staal, A., Hantson, S., Holmgren, M., van Nes, E. H., & Scheffer, M. (2018). Remotely sensed canopy height reveals three pantropical ecosystem states: Reply. *Ecology*, *99*, 235–237.

SUPPORTING INFORMATION

Additional supporting information may be found online in the Supporting Information section at the end of the article.